# Radiobiological aspects of intraoperative tumour-bed irradiation with low-energy X-rays (LEX-IORT)

**Carsten Herskind, Frederik Wenz**

Department of Radiation Oncology, Universitaetsmedizin Mannheim, Medical Faculty Mannheim, Heidelberg University, 68167 Mannheim, Germany
*Corresponding to:* Dr. Carsten Herskind. Department of Radiation Oncology, Universitaetsmedizin Mannheim, Theodor-Kutzer-Ufer 1-3, 68167 Mannheim, Germany. Email: carsten.herskind@medma.uni-heidelberg.de.

**Abstract:** Intraoperative radiotherapy (IORT) with a single high dose of low-energy X-rays (LEX) represents a major departure from conventional adjuvant radiotherapy with high-energy photons given in small daily fractions. Thus differences in beam energy, dose distribution, fraction size, dose delivery time, and time of application, may influence the biological effect of the treatment. This review presents the physical and radiobiological properties of LEX, the role of dose delivery time and fractionation, and the relative biologic effectiveness (RBE) of 50 kV X-rays from the Intrabeam machine as used for intraoperative tumour-bed irradiation. Furthermore, evidence for additional biological effects of high single doses such as non-targeted cellular effects, vascular effects, immunological effects, and cytokines, is discussed. Finally, examples of radiobiological modelling of clinical effects are given. In conclusion, the increased RBE, a small volume of high-dose irradiation, and special biological effects of high doses may contribute to the efficacy of intraoperative tumour-bed irradiation with LEX.

**Keywords:** Intraoperative radiotherapy (IORT); low-energy X-rays (LEX); relative biologic effectiveness (RBE); single high-dose

Submitted Jan 15, 2014. Accepted for publication Jan 20, 2014.
doi: 10.3978/j.issn.2218-676X.2014.01.06
**Scan to your mobile device or view this article at:** http://www.thetcr.org/article/view/2090/2755

## Introduction

Intraoperative radiotherapy (IORT) differs from conventional radiotherapy by applying a large dose in a single fraction during surgery, either as sole treatment or as an advanced boost. This potentially eliminates repopulation of residual tumour cells that may occur during wound healing before post-operative radiotherapy can begin. However, the therapeutic window between tumour control and adverse reaction in normal tissue clinically established in fractionated radiotherapy may be decreased because of the larger sensitivity to changes in the fraction size for late normal-tissue reaction.

Sources of low-energy X-rays (LEX) (<100 keV) for IORT are typically characterized by a non-uniform dose distribution, a lower dose rate, and a different radiation quality compared with conventional high-energy X-rays (MV) from linear accelerators, all of which may influence the biological effect of the treatment. In this review, the physical properties of LEX, and their relative biologic effectiveness (RBE) estimated by radiobiological modelling and experimental measurements, will be presented with emphasis on 50 kV X-rays from the Intrabeam® system (Carl Zeiss Meditec AG, Oberkochen, Germany). Furthermore, the evidence for different radiobiological effects of high single doses will be discussed and examples of modelling clinical effects in normal tissue and tumours will be given.

## Physical properties and induction of DNA damage

The propagation and interactions of photons in water or tissue depend strongly on their energy. In water, photons with energies up to a few MeV interact mainly with atomic electrons in scattering processes (Compton scattering), transferring part of their energy to an electron. At energies below approximately 100 keV, complete absorption of the energy with transfer of its energy to the photon (photoelectric

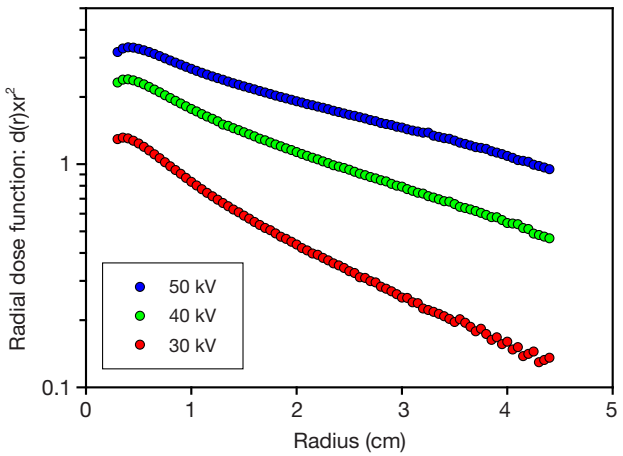


**Figure 1** Radial dose function, $d(r)\times r^2$ in water for 30-50 kV X-rays from the Intrabeam® machine without an applicator. The unit is (Gy/min) × $cm^2$ and the dose rate of the source increases with the operating voltage. $d(r)\times r^2$ is proportional to $e^{-(\mu\times r)}$ and the attenuation coefficient μ is derived from the negative slope of $\ln[d(r)\times r^2]$. The attenuation coefficient increases with decreasing photon energy. The flat slope close to the point source is due to geometrical factors. The reduced steepness at distances larger than 0.5-2 cm is evidence of beam hardening.

effect) becomes increasingly important. The probability of an interaction increases strongly with decreasing energy of the photon, especially below 25-30 keV where the photoelectric effect dominates over Compton scattering. An important property of LEX is their stronger absorption and lower penetration compared with conventional high-energy beams. Thus a larger proportion of the dose to an irradiated tissue volume is deposited close to the source. The removal of photons with distance, r, travelled in the medium is called attenuation ("thinning") of the beam. The decrease in intensity is described by the factor, $e^{-\mu\times r}$ where μ is the attenuation coefficient. The attenuation coefficient increases with decreasing photon energy (1).

The photon spectrum of X-rays ranges from the maximum energy (e.g., 50 keV) defined by the voltage of the source (e.g., 50 kV) down to almost zero energy. The attenuation coefficient increases more steeply with decreasing photon energy below 25-30 keV, and thus lower photon energies are filtered more strongly than higher energies, leading to "hardening" of the beam energy spectrum with depth in the medium. In conventional X-ray tubes and linear accelerators, metal filters remove the lowest photons energies that would otherwise be absorbed preferentially in the upper layers of the skin. At energies above 30-50 keV, beam hardening is more moderate because the attenuation coefficient decreases less steeply with increasing photon energy.

The Intrabeam machine emits a nearly isotropic field of 30-50 kV X-rays from a point source (2,3). Because of the spherical propagation, the intensity decreases as $1/r^2$ with distance from the source, r, if no attenuation occurs (i.e., in vacuum). If the beam interacts with water or tissue the beam intensity is decreased further by the attenuation factor, $e^{-\mu\times r}$. Electrons released by low-energy photons (<100 keV) have ranges shorter than 0.1 mm in water (4) and thus dissipate their energy locally. Therefore, if d(r) is the depth dose as function of distance, r, from the source, the radial dose function, $d(r)\times r^2$ essentially shows the decrease in beam intensity due to attenuation only. Hence, for a given photon energy the radial dose function should be a straight line in a semi-logarithmic diagram, with slope –μ. *Figure 1* shows this function in water for the Intrabeam source operated at 30, 40, and 50 kV. It is seen that the dose rate increases and that the steepness of the slope (attenuation coefficient) decreases as the operating voltage is increased. Photon spectra for 40 kV show that energies below 30 keV are strongly attenuated even by 5-20 mm of water (2). In *Figure 1*, the steeper slopes close to the source with a decrease in the steepness at >5-20 mm is evidence of beam hardening.

The kinetic energy of the free electrons produced by interaction of the photons is lost in ionisation and excitation events while slowing down in the medium. In water, one ionisation is produced per 20-25 eV of energy lost by the electron (5). The mean distance between ionisations is longer for high energy electrons and decreases as the electron slows down. Overall, however, electrons produce sparse ionisation tracks as opposed to the dense ionisation tracks of heavier charged particles such as α-particles and carbon ions. Different radiation qualities are characterized by the ionisation density. The linear energy transfer (LET) is defined as the mean energy deposited per track length and is measured in keV/μm. Thus sparsely ionizing photons and electrons are termed low-LET radiations whereas densely ionizing particles are high-LET radiations. The LET of photons varies with the energy, e.g., 0.2 keV/μm for 1.25 MeV photons from $^{60}$Co, and 4-6 keV/μm for 40 and 10 keV monoenergetic photons, respectively (6,7). It is important to note that this is at least an order of magnitude lower than typical high-LET values of 50-200 keV/μm for α-particles and heavier ions although the tracks of protons and very energetic low-Z ions can have lower LET values.

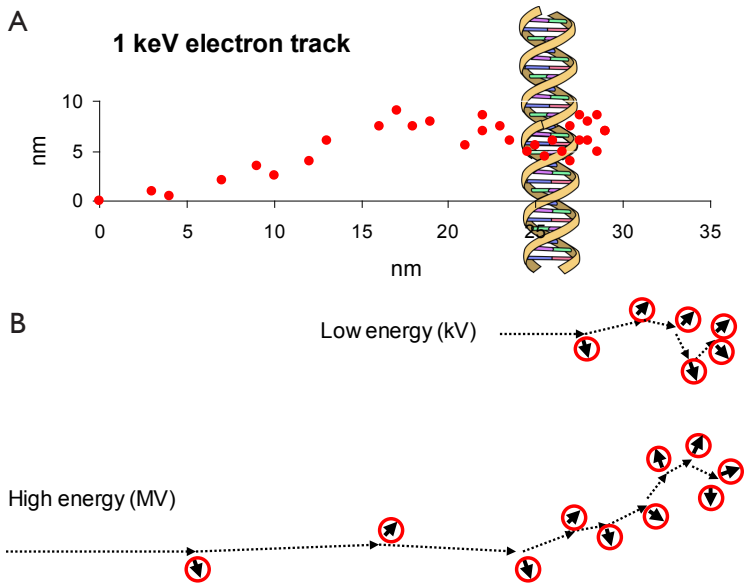


**Figure 2** (A) Schematic representation of the ionisation track of an electron with residual energy of 1 keV. The ionisation density increases towards the end of the track where it can induce double strand breaks (DSBs) and complex clustered damage in DNA; (B) Schematic representation of electron track ends (arrows in circles) similar to (A) produced by low-energy and high-energy photons (kV and MV X-rays, respectively). The dotted lines represent track segments with more widely spaced (sparse) ionisations (not drawn to scale). Low-energy X-rays deposit a larger proportion of dose in track ends than high-energy X-rays and thus produce more lethal damage per unit dose (Gy).

Radiation-induced ionisations in the nuclei of living cells result in the induction of base damage, single-strand breaks (SSBs) and double-strand breaks (DSBs) in DNA. However, only a minor fraction of the ionisations occur directly in DNA. Ionisation of water results in formation of highly reactive free radicals characterized by the presence of an unpaired electron: hydroxyl radicals (OH), hydrogen radicals (H), solvated electrons ($e_{aq}^-$), and superoxide radicals ($O_2^-$). Induction of DNA damage by radiation-induced free radicals is called "indirect action". The OH radical is the most important radical for induction of DNA strand breaks (8) but only OH radicals formed in the immediate vicinity of the DNA molecule contribute to the damage because OH radicals formed elsewhere will react with amino acids, carbohydrates and other molecules. Thus, the vast majority of the ionisations in a cell do not damage DNA. For low-LET radiation, the ratio of indirect to direct action is approximately 3:1 whereas damage by high-LET radiation is induced almost exclusively by direct action.

*Figure 2A* shows schematically the ionisations induced by a 1 keV electron, representing the end of an electron track. A small fraction of unrepaired DSBs and complex damage is considered to be the important types of lethal lesions whereas SSBs and base damage are essentially completely repaired. DSBs are formed predominantly by the clusters of ionisations at the track ends whereas base damage and SSBs can also be induced by more sparse ionisations along the track. The major difference between low-energy and high-energy X-rays is that track ends of the electrons produced by the interactions of the photons make up a larger proportion of the dose delivered by LEX (9,10) (*Figure 2B*). Thus the types of lethal lesions are the same but the dose required to produce a certain number of lethal lesions will be smaller for low-energy than for high-energy X-rays.

## Cell inactivation, recovery, and fractionation

The study of clonogenic cell survival *in vitro* has led to the notion that damage can be either irreparable resulting in a lethal lesion, or may be repairable in which case a lesion may or may not become lethal depending on the circumstances. The surviving fraction (SF) is determined as the ratio of colonies formed per cell from single cells in irradiated and unirradiated cultures. For low-LET radiation a semilogarithmic plot of SF versus dose yields a downward bending curve for most cell types (*Figure 3A*). Several mechanistic models have been proposed to explain the curve shape, postulating interaction of sublethal damage

 

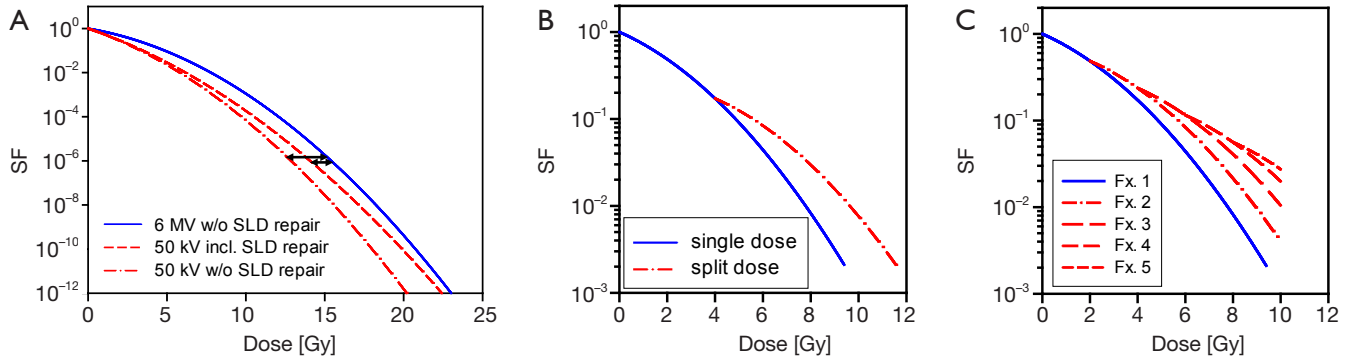


**Figure 3** (A) Linear-quadratic (L-Q) curves for surviving fraction (SF) of clonogenic cells as function of dose after irradiation with 6 MV and 50 kV X-rays. For acute irradiation (high dose rate, no sublethal damage (SLD) repair), the L-Q formalism predicts a steeper initial linear slope for low-energy X-rays. For protracted irradiation (reduced dose rate, repair of SLD during irradiation), the SF increases at higher doses. The arrows indicate isoeffective doses for calculation of the relative biologic effectiveness (RBE). The L-Q formalism predicts that RBE decreases with increasing dose; (B) Survival curves for single-dose and split-dose irradiation. If full recovery is allowed to take place after the first dose of 4 Gy, the survival curve for the second dose will be a parallel shifted curve with shape identical to the single-dose curve; (C) Survival curves for fractionated irradiation will all reproduce the initial part of the single-dose curve. If d=2 Gy fractions are repeated, the fractionated survival curve will be linear in the semilogarithmic plot.

(SLD), misrepair of potentially lethal lesions, or saturation of the repair system (11). However, most of these models lead to similar mathematical formalisms which can generally be expressed in linear-quadratic form, i.e., as a 2nd order polynomial (12):

$$\ln(SF) = -(\alpha D+\beta D^2) \quad [1]$$

The ratio of the linear and quadratic coefficients, α/β, describes the degree of curvature. For moderate values up to α/β=2-10 Gy, a shoulder is observed while at larger values (α/β→∞) the survival curve becomes increasingly linear. Importantly, the curvature is not due to SSBs induced on opposite strands by individual tracks, combining to form a DSB. Monte-Carlo calculations have shown that the energy deposition required for DSB production is due to single tracks and that the probability of two tracks depositing this energy in the relevant target volume is negligible at doses <$10^3$ Gy (13). Secondly, a simple argument shows that individual SSBs are too far apart at clinically relevant doses. Typical low-LET radiation produces ~1,000 tracks and ~1,000 SSB in the nucleus per Gy deposited (6). Since the human genome contains approximately $3\times10^9$ base pairs (bp), the mean distance between SSBs on opposite strands after a dose of 1 Gy will be approximately $2\times3\times10^6$ bp. Therefore, even doses of 20-30 Gy are insufficient to induce two SSBs close enough (≤10 bp) to form a DSB. Finally, treatment of cells with $H_2O_2$ concentrations inducing random SSBs at levels comparable to clinical doses of ionizing radiation does not produce significant numbers of DSBs (14).

In general, the linear component is interpreted as being due to irreparable, lethal lesions whereas the quadratic component represents the lesions that may potentially be repaired. Therefore, the radiation quality is considered to modify the linear coefficient α (15) while the effect of irradiation time and dose rate on repair is taken into account as a time factor G(T) in the quadratic term (16):

$$\ln(SF) = -[\alpha D+G(T)\beta D^2] \quad [2]$$

where 0<G(T)<1 for protracted irradiation. Thus the L-Q formalism predicts that α affects low doses while G(T) should affect higher doses (*Figure 3A*).

If a dose is split into two fractions separated by a time interval, recovery between the two fractions will result in the formation of a new shoulder on the survival curve. For a time interval long enough to ensure maximal recovery (usually 24 h), the second survival curve will exactly reproduce the shape of the curve for single-dose irradiation, i.e., G(T) =1 (*Figure 3B*). This forms the basis for fractionated irradiation, and the L-Q expression for n fractions of fraction size d [not the radial dose function, d(r)] can be written

$$\ln(SF) = -n(\alpha d+\beta d^2) = -(\alpha D+\beta dD) \quad [3]$$

where D= nd is the total dose. The condition that two different fraction schemes will produce the same biological effect, (i.e., will be "isoeffective") is

 

$$(\alpha D_2+\beta d_2 D_2) = (\alpha D_1+\beta d_1 D_1) \quad [4]$$

which may be rearranged to give

$$D_2=D_1(d_1+\alpha/\beta)/(d_2+\alpha/\beta) \quad [5]$$

or

$$D_2=D_1[1+d_1/(\alpha/\beta))/[1+d_2/(\alpha/\beta)] \quad [6]$$

Frequently, the equivalent dose for a standard scheme given in 2 Gy daily fractions is used as a clinically relevant reference (*Figure 3C*). In this case, $d_2$=2 Gy is inserted to calculate the isoeffective dose, $D_2$= EQD2. This has also been termed the "normalized total dose" (17).

Dividing Eq. [3] by –α gives –ln(SF)/α which is termed the "Biologically Effective Dose" (BED) and is equal to D[1+d/(α/β)], i.e., the numerator on the right hand side of Eq. [6] (18,19). Therefore, comparisons of BED values are only valid for a specific biological end point for which the values of α and α/β are constant, and consequently BED values for tumour control and late normal tissue reaction are not comparable. For this reason, the α/β value should always be indicated, e.g., $BED_{\alpha/\beta=10\ Gy}$. Furthermore, the classic BED expression cannot be used for different radiation qualities (different α) and a modification of the BED expression must be used (20,21). Importantly, BED cannot be measured directly since it represents the total dose for irradiation with infinitely small fraction size with full recovery between fractions (16-24 h) which obviously is impractical. Therefore, comparisons of clinically relevant EQD2 values are preferred (19). Caution is warranted when evaluating published studies because the terminology used in the literature is not always consistent. Thus BED is sometimes termed "biologically *equivalent* dose", and $BED_2$ has been used to indicate the biologically *equivalent* dose given in 2 Gy fractions, i.e., EQD2, rather than the "biologically *effective* dose calculated with α/β=2 Gy".

The L-Q expression for fractionated irradiation is frequently applied in clinical studies with fraction sizes in the range 1-4 Gy, and is considered valid up to d=8-10 Gy. However, whether it may be applied in IORT and stereotactic ablative radiotherapy (SABR, including stereotactic body radiotherapy and stereotactic radiosurgery), where single doses can be 20 Gy and higher, is controversially debated (22,23). The main arguments for using the L-Q formalism are its presumed mechanistic basis, a good fit of cell survival curves up to 15 Gy, and the isoeffect relationship for normal tissue reaction (22). On the other hand, it is argued that the L-Q formalism overestimates cell inactivation at higher doses *in vitro* but may underestimate clinical effectiveness *in vivo* because of effects on the vasculature, and that resistant subpopulations of cancer stem cells or hypoxic cells may become important (23). In this discussion, it should be noted that the central parameter α/β in the clinical application of the L-Q expression is not determined by an independent method such as a cell survival curve but by fitting data from fractionation studies. Late normal-tissue reaction may not even be directly linked with clonogenic cell inactivation but may depend on cytokines or other radiation-induced signals (24). Thus individual patients' risk for developing late reaction show no correlation between different late endpoints suggesting that the mechanisms are different (25). Furthermore, no significant correlation was found between the radiosensitivity of individual patients' fibroblasts and the patients' risk of developing subcutaneous fibrosis (26-28). In spite of the lacking mechanistic basis, the L-Q expression has proven useful for late normal-tissue reactions.

Clinical data for SABR support the clinical efficacy of very large doses per fraction towards metastatic tumours in the liver and lung (29-31) or primary NSCLC (32). Despite heterogeneous doses, fractionation schemes, tumour volumes and entities, 70-90% local control is achieved for doses equivalent to EQD2 in the range 50-100 Gy, while >90% may be achieved for EQD2 >100 Gy (32-34). This is at least as good as control rates from conventional fractionated radiotherapy. A comparison of SABR applied as a single dose or in three equal fractions shows no indication that single doses should be less efficient than three fractions [*Figure 4* and (57)]. Taken together, these data do not support a significant break-down of the L-Q expression at high doses per fraction.

Modifications of the L-Q formalism to increase SF values at high doses have been proposed, which lead to higher estimates of single doses isoeffective with conventional fractionated radiotherapy (58-61). Although, for a given single dose, these models will result in a lower estimate of the equivalent conventional total dose, fitting the universal survival curve (60) and the L-Q model (34) to current clinical data did not show a significantly better fit for either model. Therefore, in the absence of a validated superior model it seems reasonable to use the L-Q model for initial guidance to estimating isoeffective doses of single-dose IORT up to fraction sizes of 15-20 Gy. However, careful monitoring and long-term follow up are always mandatory when new clinical fraction schemes are introduced.

## Relative biologic effectiveness (RBE)

As described above, radiation qualities differ with respect to their biologic effectiveness. The RBE is defined as the

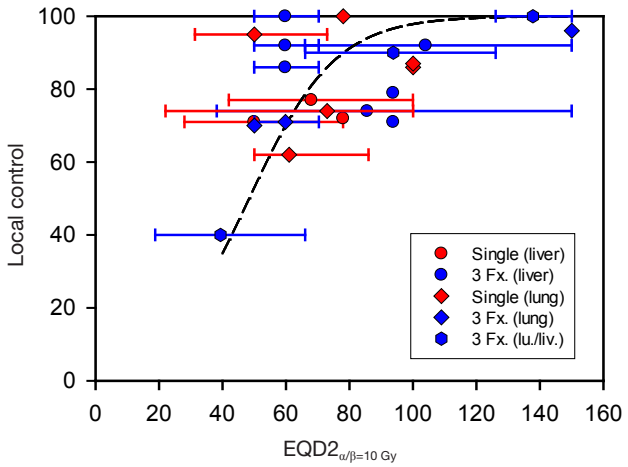


**Figure 4** Local control (1-2 yrs follow-up) for metastases in the liver and lung treated with a single dose or 3 equal fractions of stereotactic ablative radiotherapy (SABR). The equivalent dose given in 2 Gy fractions was calculated for α/β=10 Gy ($EQD_{2\alpha/\beta=10\ Gy}$). The broken line is for guidance of the eye only, and does not imply an exact statistical fit of a dose-response curve. The data were selected from studies on liver metastases (35-44) reviewed by Hoyer *et al.* (30) and lung metastases (45-56) reviewed by Siva *et al.* (29).

ratio of doses of a reference radiation (usually high-energy photons, such as $^{60}$Co γ-rays or 4-6 MV X-rays) and the test irradiation: RBE $=D_{ref}/D_{test}$. According to the L-Q formalism the radiation quality increases the slope of the survival curve at low doses while repair during protracted irradiation reduces the slope at higher doses (cf. *Figure 3A*). Consequently, RBE is predicted to reach its maximum value for D→0 Gy where $RBE_{max}=\alpha_{ref}/\alpha_{test}$ and to decrease with increasing dose (16,62).

The RBE of LEX from the Intrabeam machine has been modelled for the naked source operated at 40 kV relative to protracted irradiation with $^{60}$Co γ-rays based on certain assumptions and was estimated for different depths in water using α/β=8 Gy for the reference radiation (16). $RBE_{max}$ in the low-dose limit (D→0 Gy) decreased from 3.05 for the naked source to 2.44 in 20 mm depth owing to beam hardening with increasing depth. At a dose of 12.5 Gy, values of RBE varied between 1.53 and 1.40. Experimental data for the naked source operated at the same voltage yielded values of 3.3 and 1.9 relative to 6MV X-rays for cell inactivation at survival levels SF=0.5 and SF=0.05, respectively, representing the dose range 1-4 Gy (63).

Following a slightly modified modelling approach, the RBE for irradiation with 50 kV X-rays from Intrabeam with spherical applicators for tumour bed irradiation was calculated as function of distance from the applicator surface relative to acute irradiation with reference radiation (62). Using α/β=3 Gy for late-reacting normal tissue, this yielded RBE values in the range 1.15-1.5 at 0-10 mm distance from the applicator surface if recovery was neglected. Including the effect of recovery reduced the RBE by up to 0.2 for the high dose of 20 Gy at the applicator surface. The largest reduction was for large-diameter applicators which require longer irradiation times. For α/β=10 Gy, considered typical for many tumours, RBE varied in the range 1.2-1.8 including the effect of recovery during protracted irradiation. However, recent hypofractionation studies in early breast cancer suggest that α/β may be closer to 4 Gy (64-66) which would bring the L-Q estimate of RBE closer to that of normal tissue. Experimental determination of RBE for cell inactivation *in vitro* was performed for different cell types irradiated with Intrabeam (50 kV) in a water-equivalent tumour-bed phantom relative to irradiation with acute doses of 6 MV X-rays. At 8 mm distance from the surface of a 4.0 cm diameter applicator, a mean value of RBE =1.35 with confidence interval 1.2-1.5 was determined in the dose range 1-4 Gy. This value was similar to the RBE of 50 kV X-rays with 1 mm Al filter from a surface radiotherapy machine (Dermopan, Siemens) (67) and was also consistent with previous data for experimental X-ray sources in the 50-70 kV range using 0.7-1.5 mm Al filtering (68-70). The higher RBE (1.9-3.3) described above for the 40 kV Intrabeam source without an applicator (63), indicates the importance of beam energy and filtering for the RBE. No significant dependence of the RBE on dose was observed at 8mm depth in the water-equivalent phantom in contrast with the predictions of the L-Q formalism. Similar evidence for the absence of dose dependence has been found in previous studies of LEX (68-71). Further support that changes in radiation quality may affect not only the linear coefficient, α, but also β in the L-Q formalism comes from some studies with ultrasoft X-rays and high-LET radiation (72,73).

In the experimental study by Liu *et al.* (67) the RBE was found to decrease at larger distance (12.7 mm) from the applicator surface where the dose rate was reduced. This may be due to the effect of continuous induction and decay of SLD during irradiation, additional beam hardening in the water-equivalent phantom, or a combination of both. According to the L-Q formalism, a reduced dose rate should result in an increase of SF and thus a decrease in RBE at higher doses of 50 kV X-rays (*Figure 3A*). However,

 

the decrease in RBE was observed even at low doses [(67) and Liu *et al*., unpublished data] which might suggest that part of the low-dose damage is repairable. On the other hand, detailed examination of the radial dose function for Intrabeam with applicators for tumour bed irradiation (not shown) suggests that for 3.5-5.0 cm diameter applicators, beam filtering in the applicator material is less than in water, and that hardening of the beam in water occurs at distances up to 5-15 mm from the applicator surface. By contrast, applicators with 1.5-3.0 cm diameter appear to filter the beam more strongly than water due to the beam hardening effect of an aluminium filter built into the smaller applicators. Thus, the radial dose functions indicate beam *softening* in water as the beam exits the applicator. This implies that the RBE at the applicator surface may be lower for 1.5-3.0 cm applicators and higher for 3.5-5.0 cm applicators than measured in the water-equivalent phantom at 8mm distance from the surface of the 4.0 cm applicator.

## Biological effects of high single doses

Most radiobiological studies on cells have been performed in the dose range 1-8 Gy where cellular radiation effects, including clonogenic inactivation and survival can be studied conveniently. However, some evidence suggests that large single doses as used in IORT may produce different effects from those seen after conventional fraction sizes (74-76).

The saturated repair model has been proposed to explain the curved shape of the survival curve for low-LET radiation (77). Using DNA repair foci such as phosphorylated histone variant γH2AX to detect DSBs in intact cells, DSB induction is proportional to dose in the 0-3 Gy range but increases less steeply at higher doses (14,75,78). Some data indicate a dynamic repair response (i.e., proportional to dose) at low doses with increasing saturation at higher doses (75) [Liu Q., PhD thesis; Zhang B., PhD thesis]. However, whether this simply reflects slower kinetics or indeed more residual damage is not clear. Nevertheless, it seems conceivable that repair saturation might play a role for radiation-induced chromosome instability and cell lethality after high doses.

It is frequently argued that the shape of the survival curve deviates from the L-Q shape and is more linear at higher doses and that the L-Q formalism might overestimate cell killing (79). However, SFs smaller than $10^{-3}$-$10^{-4}$ are notoriously difficult to measure in human cells because few colonies are formed *in vitro*. Furthermore, the results may be confounded by artefacts such as culture conditions, experimental design, and reduced colony sizes. Recent evidence suggests that non-targeted effects may contribute to clonogenic cell inactivation at higher doses. Thus reduced SF values of breast cancer cells after a dose of 12 Gy were found when the cell density in the irradiated culture was increased (80). This represents a so-called "cohort" effect (81) and increased the downward curvature of the survival curve. Part of the dose-dependent effect was shown to be mediated by a transferrable factor that induced sustained expression of γH2AX foci in unirradiated cells, suggesting that genomic instability may be involved (80). The transferrable factor did not appear to be TGF-β1 or 36 cytokines tested in an antibody array, and remains to be identified.

Single doses of 10-15 Gy have been shown to inhibit the growth of fibrosarcoma and melanoma tumours in mice by releasing the pro-apoptotic second-messenger ceramide from sphingomyelin in membranes of endothelial cells. The ceramide release was mediated by acid sphingomyelinase (asmase) and resulted in apoptosis of endothelial cells (82). The endothelial apoptosis interacted with radiation effects on tumour clonogens because radiation-induced tumour growth inhibition was absent in asmase-deficient host mice, even though the tumour was asmase positive. Preliminary evidence suggested that endothelial apoptosis might radiosensitize tumour cells by interfering with DSB repair (83). Asmase activation and apoptosis could be suppressed by VEGF or FGF2, and the suppression was reversed by adding pro-apoptotic C16-ceramide (84). At higher doses (18-20 Gy), the target switched from endothelial cells to stem cells by inducing ceramide synthase resulting in *de novo* ceramide synthesis in stem cells (85). Radiation-induced DSBs upregulated CerS and this pathway contributed to inactivation of clonogens in the crypt cell assays (86). In HeLa cells, apoptosis seemed to be regulated by the balance between pro-apoptotic C16:0 ceramide and anti-apoptotic C24:0 and C24:1 ceramide (87). Interestingly, these ceramides, and CerS6 and CerS2 which are involved in their synthesis (88), were upregulated in primary breast cancer tissue (89). Thus it seems a distinct possibility that ceramide synthesis may contribute to inactivation of breast cancer stem cells by high single doses.

High-dose irradiation of the microvasculature may lead to adhesion of platelets to endothelial cells with formation of thrombi (90). Recently, irradiation with a single dose of 30 Gy was shown to lead to persistent thrombi formation over 24 h in a mouse tumour model although most resolved

 

again with time (91). Thus coagulation involving endothelial cells of the tumour microvasculature may contribute to enhance the biological effect of a high single dose of IORT.

Increasing evidence suggests that immunological anti-tumor effects may contribute to the effects of high-dose irradiation. Radiotherapy may create a tumour microenvironment conducive of an immunogenic response (92-94). Single doses of 10-25 Gy induced long-term expression of MHC-I in tumour cells resulting in antigen presentation and enhanced recognition by cytotoxic T-lymphocytes (95). Upregulation of MCH-I expression was mediated by radiation-induced IFN-γ in a murine melanoma model (96). Furthermore, high doses of radiation may increase lysis of tumour cells thereby releasing tumour-associated antigens (TAA) which can be taken up by professional antigen presenting cells (APC) such as dendritic cells and macrophages (97,98). Activation of APC is stimulated by pro-inflammatory cytokines, and the activated APC migrate to the tumour-draining lymph node where they activate $CD8^+$ "cytotoxic" T-cells (CTL). Irradiation increases the number and activity of APC in mice, and stimulates trafficking of CTL into the tumour (96,99). Efficient antigen presentation by professional APC requires expression MCH-II and co-stimulatory molecules such as B7 activating $CD4^+$ "helper" T-cells. A pro-inflammatory Th1 response in $CD4^+$ T-helper cells in turn stimulates activation of $CD8^+$ cells, and the cytotoxic immune response was strong enough to reduce relapse and eradicate metastases in a mouse melanoma model (100). However, many cancer cells are compromised in their expression of MHC-I (98), and radiation-induced enhancement of $T_{reg}$ may suppress a tumour-specific immune response (101). Therefore, the optimal fraction size and sequence for the immune response needs to be worked out in a clinical setting (102). Conceivably, this may have to be done for each tumour type and anatomical site. If irradiation of the tumour draining lymph nodes influences the immune response, differences in dose distributions and treatment volumes between IORT and conventional WBRT could turn out to be important.

A direct role of cytokines in invasion and migration of tumour cells was suggested by a study on breast cancer patients undergoing IORT according to the TARGIT protocol (103,104). Previously, it has been found that wound fluid collected from breast cancer patients stimulates proliferation of breast cancer cells, in particular those expressing receptor tyrosine kinase HER2 (105). Stimulation of proliferation by wound fluid from breast cancer patients was verified in 2-dimensional cell culture of HER2+ and HER2- cells but no difference was found between wound fluids from patients irradiated according to the TARGIT protocol and unirradiated control patients (103). However, treatment of MCF7 breast cancer cells with wound fluid in 3-dimensional (3-D) Matrigel® cultures resulted in an apparent increase of colony size for wound fluid collected from unirradiated but not from IORT treated patients. Furthermore, IORT to the tumour bed abrogated the stimulatory effect of wound fluid on migration and invasion observed with wound fluid from unirradiated patients. Since cytokine levels were differentially regulated (20 down and 10 up) it was suggested that changes in molecular composition and biological activity of wound fluid by intraoperative tumour-bed irradiation might contribute to reducing the recurrence rate (103).

A schematic model of the different biological effects of high single doses is shown in *Figure 5*.

## Modelling clinical effects of IORT

When introducing a new radiotherapy modality like IORT with LEX, it is important to estimate the anticipated biological effects on normal tissue and tumour cells based on previous clinical data from fractionated radiotherapy. RBE as function of dose may be estimated using the L-Q formalism with various assumptions regarding RBE and the effect of repair (62). The RBE is then used to convert the single dose to the isoeffective single dose of high-energy X-rays. For pneumonitis, the dose-response relationship is known for single-dose irradiation (106) and thus the risk of pneumonitis can be estimated as function of dose from the applicator surface. In most cases, however, the dose-response relationship is known only for fractionated radiotherapy and the L-Q formalism is used to convert the single dose of reference radiation to the isoeffective dose of fractionated radiotherapy for which clinical data are available.

The dose response for pneumonitis after single-dose irradiation shows an ED50 (dose to produce effect in 50% of the patients) of 9.3 Gy (106). Modelling pneumonitis of the lung as function of dose indicated that the risk of pneumonitis is limited to approximately 8-12 mm from the applicator surface, depending on the applicator size and the assumptions regarding the RBE (62). Thus the lung is shielded by the thickness of the thorax wall.

The ED50 for subcutaneous fibrosis has been estimated at EQD2~50 Gy for a standard fractionation scheme with 2-Gy fractions or approximately 14 Gy for single-dose

 

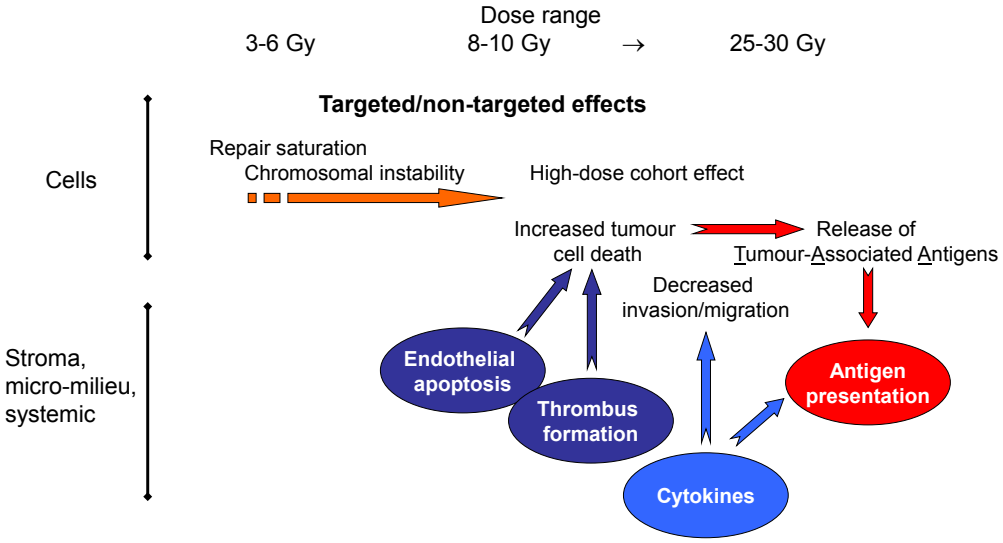


**Figure 5** Schematic model of special biological effects of high single doses at the cellular, tissue, and systemic levels.

irradiation (62,107). Modelling predicts that fibrosis should be limited to 3-5 mm if IORT is given as sole treatment (62). Normal tissue can tolerate higher doses if the irradiated volume is small (108), and this may explain the very low rate of fibrosis when IORT is applied as sole radiation treatment. IORT may also be applied as an advanced boost in combination with a course of post-operative external-beam radiotherapy with slightly reduced dose, e.g., to 46 Gy in 2-Gy fractions. The IORT boost adds a contribution to EQD2 of typically approximately 15 Gy at 10 mm depth, i.e., similar to a conventional boost with external beam irradiation. Although the EQD2 close to the applicator will be considerably higher, moderate to severe fibrosis is observed only in about a third of the patients (109,110) [E. Sperk, personal communication]. Thus the rate of fibrosis is similar to rates observed after a postoperative boost with an external beam (66,111-113).

The steep radial dose gradient of 50 kV X-rays around spherical applicators for tumour-bed irradiation has raised concerns that the dose at 10 mm distance will not be sufficient for tumour control. Inserting cell survival parameters obtained for typical breast cancer cell lines *in vitro*, into the L-Q expression indicates SF~$10^{-2}$ at 10 mm depth in the tumour bed (62). Obviously, this would inactivate only a relatively small number of tumour stem cells. However, it is important to note that the solid tumour has been removed by surgery so, provided that no residual tumour mass has been left, it may be assumed that only a small number of recurrence-forming tumour foci will be present. Furthermore, approximately 70% of early breast cancer patients will not develop recurrence even when adjuvant radiotherapy is omitted. Therefore, the remaining 30% of the patients are likely to have only a single cluster of recurrence-forming tumour cells in the tumour bed that will vary in size by several orders of magnitude from only a few to perhaps more than tens of thousands cells. This implies that the clinical dose response curve will not show the sigmoidal form typical for solid tumour but may start at ~70% at 0 Gy with a gradual slope towards higher values (75). Furthermore, the probability of finding such recurrence-forming foci is likely to decrease with increasing distance from the excised tumour [(foci in other quadrant are usually considered new primaries (114,115)].

Modelling the risk of recurrence was performed using a clinical dose response relationship (116) based on a standard fractionation scheme and the EORTC boost study (111), and incorporating the advantage of eliminating proliferation of tumour cells between surgery and the start of post-operative, fractionated radiotherapy (117). The model calculations suggested that the EQD2 values near the applicator surface are larger than 50 Gy given in a standard course of whole-breast radiotherapy. Thus close to the applicator surface, tumour foci would have a lower risk of recurrence compared with a uniform dose distribution while the risk of recurrence would increase with distance from the applicator (depth in the tumour bed). This implies that, within a certain distance, the mean risk of recurrence for a cohort of patients would be the same as for a uniform

 

**Table 1** Summary of radiobiological factors contributing to the efficacy of intraoperative tumour-bed irradiation with low-energy X-rays

| Summary and conclusions |
|---|
| Increased relative biologic effectiveness (RBE) |
| RBE is increased (>1) for low- (kV) relative to high-energy (MV) X-rays. The RBE at a given tissue depth (distance from the applicator surface) may be independent of dose. Protracted irradiation delivery time (i.e., low dose rate) may affect repair not only at higher doses (quadratic component) but also at low doses. Longer irradiation times, and beam hardening in the tissue (for 3.5-5.0 cm spherical applicators) may result in decreasing RBE values with increasing tissue depth but will depend also on filtering by the applicator |
| Lack of fractionation |
| Fractionation protects late-reacting normal tissue relative to tumour cells, and allows reoxygenation of hypoxic tumour cells. However, the smaller therapeutic window of single dose of intraoperative radiotherapy (IORT) is moderated by the relatively low $\alpha / \beta$ ratio (~4 Gy) for breast tumours. Furthermore, hypoxia is unlikely to be important in residual foci of tumour cells. Clinical data for SBRT with 1-3 fractions support the use of the L-Q expression as an initial guide to isoeffective doses |
| Biological effects of high single doses |
| Genetic (chromosomal) instability may inhibit clonogenic proliferation, and non-targeted effects may contribute to radiation-induced cell inactivation at higher doses. Ceramide-mediated apoptosis of endothelial cells activated by asmase may radiosensitize tumours in the dose range 10-15 Gy while induction of ceramide synthesis in tumour cells may contribute to inactivation at higher doses (>18-20 Gy). High dose irradiation may act as an adjuvant for immune reactions against tumour cells, and may inhibit the pro-migration and pro-invasion cytokine profile in the microenvironment during wound healing |
| Non-uniform dose distribution |
| The low risk of recurrence of tumour cell foci in the high-dose region close to the applicator surface is estimated to partly compensate the increased risk of recurrence at larger distances, defining a 'Sphere of Equivalence' with a uniform dose distribution from an external beam. The risk of adverse reactions after IORT with low-energy X-rays is limited by the small volume of the high-dose region |

dose distribution from an external beam of high-energy X-rays. This spherical shell defines a new target volume concept termed the "*Sphere of Equivalence*" (116). Model calculations estimated that this may extend up to a distance of 8-10 mm from the applicators surface. Furthermore, the calculations were fairly robust towards changes in the assumptions of the model. Theoretically, the size of the *Sphere of Equivalence* may be increased by fractionation designed to be isoeffective for late normal tissue damage. Thus the therapeutic window is predicted to be increased by APBI in ten fractions in a perioperative setting (107). However, this may compromise the advantage of IORT in eliminating tumour cell proliferation between surgery and radiotherapy as suggested by the inferior outcome in the TARGIT trial of patients receiving post-pathology IORT in a second surgical session (118).

As the number of cancer survivors increases owing to earlier and better diagnostics and improved therapy options, very late effects such as the development of 2$^{nd}$ primary cancers after therapy is becoming more important. Although the risk is small (119), modelling calculations based on the dose distributions suggest that IORT with LEX as given in TARGIT may decrease the risk even further (120).

## Summary and conclusions

Radiation therapy is an important adjuvant therapy to surgery in the treatment of malignant tumours. Applying radiotherapy as IORT to the tumour bed during surgery eliminates repopulation of tumour cells which otherwise increases the load of tumour cells during wound healing before conventional postoperative radiotherapy can begin. Thus the isoeffective dose of IORT to achieve identical tumor control rates may be smaller. On the other hand, giving a single nonuniform dose of LEX instead of a conventional course of fractionated RT high-energy X-rays with uniform dose distribution may reduce the therapeutic window between tumour control and late tissue reaction. Furthermore, lower doses at large distance from the applicator might compromise control of residual tumour cells.

However, a number of factors work in the favour of IORT with LEX (LEX-IORT). For breast cancer, residual cancer cells after removal of the tumour are likely to be present as single foci with varying cell numbers so that

 

even small doses should contribute to reducing the risk of recurrence. The RBE is increased so that the equivalent dose of reference radiation will be higher than the physical dose. Furthermore, the difference in sensitivity of tumour and normal tissue to changes in fraction size may be smaller than previously thought, thus helping to preserve a therapeutic window. Furthermore, biological effects of high single doses may be different from those observed at low dose per fraction which may compensate the potential disadvantages of high single doses. Clinical modelling of tumour-bed IORT in breast cancer suggests that high doses close to the applicator surface produce a *Sphere of Equivalence* with external beam radiotherapy, and that the small volume of normal tissue exposed to high doses limits adverse normal-tissue reaction (*Table 1*).

## Acknowledgments

*Funding:* Carl Zeiss Meditec AG supports radiobiological research at the Universitaetsmedizin Mannheim.

## Footnote

*Provenance and Peer Review:* This article was commissioned by the editorial office, *Translational Cancer Research* for the series "Intraoperative Radiotherapy". The article has undergone external peer review.

*Conflicts of Interest:* Both authors have completed the ICMJE uniform disclosure form (available at http://dx.doi.org/10.3978/j.issn.2218-676X.2014.01.06). The series "Intraoperative Radiotherapy" was commissioned by the editorial office without any funding or sponsorship. FW served as the unpaid Guest Editor of the series and serves as an unpaid editorial board member of *Translational Cancer Research*. The authors have no other conflicts of interest to declare.

*Ethical Statement:* The authors are accountable for all aspects of the work in ensuring that questions related to the accuracy or integrity of any part of the work are appropriately investigated and resolved.



## References

1. Tables of X-Ray Mass Attenuation Coefficients and Mass Energy-Absorption Coefficients from 1 keV to 20 MeV for Elements Z = 1 to 92 and 48 Additional Substances of Dosimetric Interest [database on the Internet] 1996. Available online: http://www.nist.gov/pml/data/xraycoef/
2. Beatty J, Biggs PJ, Gall K, et al. A new miniature x-ray device for interstitial radiosurgery: dosimetry. Med Phys 1996;23:53-62.
3. Dinsmore M, Harte KJ, Sliski AP, et al. A new miniature x-ray source for interstitial radiosurgery: device description. Med Phys 1996;23:45-52.
4. Meesungnoen J, Jay-Gerin JP, Filali-Mouhim A, et al. Low-energy electron penetration range in liquid water. Radiat Res 2002;158:657-60.
5. Vassiliev ON. Electron slowing-down spectra in water for electron and photon sources calculated with the Geant4-DNA code. Phys Med Biol 2012;57:1087-94.
6. Hall EJ, Giaccia AJ. eds. Radiobiology for the Radiologist. 7th ed. Philadelphia: Lippincott Williams & Wilkins, 2011.
7. Kellerer AM. Electron spectra and the RBE of X rays. Radiat Res 2002;158:13-22.
8. Herskind C, Westergaard O. Inactivation of a single eucaryotic gene irradiated in transcriptionally active chromatin form. Radiat Res 1986;106:331-44.
9. Goodhead DT. Models of radiation inactivation and mutagenesis. In: Meyn RE, Withers HR. eds. Radiation Biology in Cancer Research. New York: Raven Press, 1980:231-47.
10. Goodhead DT, Thacker J, Cox R. Weiss Lecture. Effects of radiations of different qualities on cells: molecular mechanisms of damage and repair. Int J Radiat Biol 1993;63:543-56.
11. Joiner MC. Quantifying cell kill and cell survival. In: Joiner M, Van der Kogel A. eds. Basic Clinical Radiobiology. Fourth ed. London: Hodder Arnold, 2009:41-55.
12. Brenner DJ, Hlatky LR, Hahnfeldt PJ, et al. The linear-quadratic model and most other common radiobiological models result in similar predictions of time-dose relationships. Radiat Res 1998;150:83-91.
13. Goodhead DT, Nikjoo H. Track structure analysis of ultrasoft X-rays compared to high- and low-LET radiations. Int J Radiat Biol 1989;55:513-29.

 

14. Löbrich M, Shibata A, Beucher A, et al. gammaH2AX foci analysis for monitoring DNA double-strand break repair: strengths, limitations and optimization. Cell Cycle 2010;9:662-9.
15. Denekamp J, Waites T, Fowler JF. Predicting realistic RBE values for clinically relevant radiotherapy schedules. Int J Radiat Biol 1997;71:681-94.
16. Brenner DJ, Leu CS, Beatty JF, et al. Clinical relative biological effectiveness of low-energy x-rays emitted by miniature x-ray devices. Phys Med Biol 1999;44:323-33.
17. Lebesque JV, Keus RB. The simultaneous boost technique: the concept of relative normalized total dose. Radiother Oncol 1991;22:45-55.
18. Fowler JF. The linear-quadratic formula and progress in fractionated radiotherapy. Br J Radiol 1989;62:679-94.
19. Joiner MC, Bentzen SM. Fractionation: the linear-quadratic approach. In: Joiner M, Van der Kogel A. eds. Basic Clinical Radiobiology. Fourth ed. London: Hodder Arnold, 2009:102-19.
20. Dale RG, Jones B. The assessment of RBE effects using the concept of biologically effective dose. Int J Radiat Oncol Biol Phys 1999;43:639-45.
21. Fowler JF. 21 years of biologically effective dose. Br J Radiol 2010;83:554-68.
22. Brenner DJ. The linear-quadratic model is an appropriate methodology for determining isoeffective doses at large doses per fraction. Semin Radiat Oncol 2008;18:234-9.
23. Kirkpatrick JP, Meyer JJ, Marks LB. The linear-quadratic model is inappropriate to model high dose per fraction effects in radiosurgery. Semin Radiat Oncol 2008;18:240-3.
24. Bentzen SM. Preventing or reducing late side effects of radiation therapy: radiobiology meets molecular pathology. Nat Rev Cancer 2006;6:702-13.
25. Bentzen SM, Overgaard M, Overgaard J. Clinical correlations between late normal tissue endpoints after radiotherapy: implications for predictive assays of radiosensitivity. Eur J Cancer 1993;29A:1373-6.
26. Johansen J, Bentzen SM, Overgaard J, et al. Relationship between the in vitro radiosensitivity of skin fibroblasts and the expression of subcutaneous fibrosis, telangiectasia, and skin erythema after radiotherapy. Radiother Oncol 1996;40:101-9.
27. Peacock J, Ashton A, Bliss J, et al. Cellular radiosensitivity and complication risk after curative radiotherapy. Radiother Oncol 2000;55:173-8.
28. Russell NS, Grummels A, Hart AA, et al. Low predictive value of intrinsic fibroblast radiosensitivity for fibrosis development following radiotherapy for breast cancer. Int J Radiat Biol 1998;73:661-70.
29. Siva S, MacManus M, Ball D. Stereotactic radiotherapy for pulmonary oligometastases: a systematic review. J Thorac Oncol 2010;5:1091-9.
30. Høyer M, Swaminath A, Bydder S, et al. Radiotherapy for liver metastases: a review of evidence. Int J Radiat Oncol Biol Phys 2012;82:1047-57.
31. Tree AC, Khoo VS, Eeles RA, et al. Stereotactic body radiotherapy for oligometastases. Lancet Oncol 2013;14:e28-37.
32. van Baardwijk A, Tome WA, van Elmpt W, et al. Is high-dose stereotactic body radiotherapy (SBRT) for stage I non-small cell lung cancer (NSCLC) overkill? A systematic review. Radiother Oncol 2012;105:145-9.
33. Boda-Heggemann J, Dinter D, Weiss C, et al. Hypofractionated image-guided breath-hold SABR (stereotactic ablative body radiotherapy) of liver metastases--clinical results. Radiat Oncol 2012;7:92.
34. Mehta N, King CR, Agazaryan N, et al. Stereotactic body radiation therapy and 3-dimensional conformal radiotherapy for stage I non-small cell lung cancer: A pooled analysis of biological equivalent dose and local control. Pract Radiat Oncol 2012;2:288-95.
35. Ambrosino G, Polistina F, Costantin G, et al. Image-guided robotic stereotactic radiosurgery for unresectable liver metastases: preliminary results. Anticancer Res 2009;29:3381-4.
36. Goodman KA, Wiegner EA, Maturen KE, et al. Dose-escalation study of single-fraction stereotactic body radiotherapy for liver malignancies. Int J Radiat Oncol Biol Phys 2010;78:486-93.
37. Herfarth KK, Debus J, Wannenmacher M. Stereotactic radiation therapy of liver metastases: update of the initial phase-I/II trial. Front Radiat Ther Oncol 2004;38:100-5.
38. Hoyer M, Roed H, Traberg Hansen A, et al. Phase II study on stereotactic body radiotherapy of colorectal metastases. Acta Oncol 2006;45:823-30.
39. McCammon R, Schefter TE, Gaspar LE, et al. Observation of a dose-control relationship for lung and liver tumors after stereotactic body radiation therapy. Int J Radiat Oncol Biol Phys 2009;73:112-8.
40. Méndez Romero A, Wunderink W, Hussain SM, et al. Stereotactic body radiation therapy for primary and metastatic liver tumors: A single institution phase i-ii study. Acta Oncol 2006;45:831-7.
41. Rusthoven KE, Kavanagh BD, Cardenes H, et al. Multi-institutional phase I/II trial of stereotactic body radiation therapy for liver metastases. J Clin Oncol 2009;27:1572-8.
42. van der Pool AE, Mendez Romero A, Wunderink W, et

 

al. Stereotactic body radiation therapy for colorectal liver metastases. Br J Surg 2010;97:377-82.
43. Wada H, Takai Y, Nemoto K, et al. Univariate analysis of factors correlated with tumor control probability of three-dimensional conformal hypofractionated high-dose radiotherapy for small pulmonary or hepatic tumors. Int J Radiat Oncol Biol Phys 2004;58:1114-20.
44. Wulf J, Guckenberger M, Haedinger U, et al. Stereotactic radiotherapy of primary liver cancer and hepatic metastases. Acta Oncol 2006;45:838-47.
45. Fritz P, Kraus HJ, Muhlnickel W, et al. Stereotactic, single-dose irradiation of stage I non-small cell lung cancer and lung metastases. Radiat Oncol 2006;1:30.
46. Guckenberger M, Heilman K, Wulf J, et al. Pulmonary injury and tumor response after stereotactic body radiotherapy (SBRT): results of a serial follow-up CT study. Radiother Oncol 2007;85:435-42.
47. Hara R, Itami J, Kondo T, et al. Stereotactic single high dose irradiation of lung tumors under respiratory gating. Radiother Oncol 2002;63:159-63.
48. Hof H, Hoess A, Oetzel D, et al. Stereotactic single-dose radiotherapy of lung metastases. Strahlenther Onkol 2007;183:673-8.
49. Milano MT, Katz AW, Muhs AG, et al. A prospective pilot study of curative-intent stereotactic body radiation therapy in patients with 5 or fewer oligometastatic lesions. Cancer 2008;112:650-8.
50. Milano MT, Katz AW, Schell MC, et al. Descriptive analysis of oligometastatic lesions treated with curative-intent stereotactic body radiotherapy. Int J Radiat Oncol Biol Phys 2008;72:1516-22.
51. Nakagawa K, Aoki Y, Tago M, et al. Megavoltage CT-assisted stereotactic radiosurgery for thoracic tumors: original research in the treatment of thoracic neoplasms. Int J Radiat Oncol Biol Phys 2000;48:449-57.
52. Okunieff P, Petersen AL, Philip A, et al. Stereotactic Body Radiation Therapy (SBRT) for lung metastases. Acta Oncol 2006;45:808-17.
53. Rusthoven KE, Kavanagh BD, Burri SH, et al. Multi-institutional phase I/II trial of stereotactic body radiation therapy for lung metastases. J Clin Oncol 2009;27:1579-84.
54. Wulf J, Haedinger U, Oppitz U, et al. Stereotactic radiotherapy for primary lung cancer and pulmonary metastases: a noninvasive treatment approach in medically inoperable patients. Int J Radiat Oncol Biol Phys 2004;60:186-96.
55. Wulf J, Baier K, Mueller G, et al. Dose-response in stereotactic irradiation of lung tumors. Radiother Oncol 2005;77:83-7.
56. Yoon SM, Choi EK, Lee SW, et al. Clinical results of stereotactic body frame based fractionated radiation therapy for primary or metastatic thoracic tumors. Acta Oncol 2006;45:1108-14.
57. Ricardi U, Filippi AR, Guarneri A, et al. Stereotactic body radiation therapy for lung metastases. Lung Cancer 2012;75:77-81.
58. Astrahan M. BED calculations for fractions of very high dose: in regard to Park et al. (Int J Radiat Oncol Biol Phys 2007;69:S623-S624). Int J Radiat Oncol Biol Phys 2008;71:963; author reply 963-4.
59. Guerrero M, Li XA. Extending the linear-quadratic model for large fraction doses pertinent to stereotactic radiotherapy. Phys Med Biol 2004;49:4825-35.
60. Park C, Papiez L, Zhang S, et al. Universal survival curve and single fraction equivalent dose: useful tools in understanding potency of ablative radiotherapy. Int J Radiat Oncol Biol Phys 2008;70:847-52.
61. Wang JZ, Huang Z, Lo SS, et al. A generalized linear-quadratic model for radiosurgery, stereotactic body radiation therapy, and high-dose rate brachytherapy. Sci Transl Med 2010;2:39ra48.
62. Herskind C, Steil V, Kraus-Tiefenbacher U, et al. Radiobiological aspects of intraoperative radiotherapy (IORT) with isotropic low-energy X rays for early-stage breast cancer. Radiat Res 2005;163:208-15.
63. Astor MB, Hilaris BS, Gruerio A, et al. Preclinical studies with the photon radiosurgery system (PRS). Int J Radiat Oncol Biol Phys 2000;47:809-13.
64. START Trialists' Group, Bentzen SM, Agrawal RK, et al. The UK Standardisation of Breast Radiotherapy (START) Trial A of radiotherapy hypofractionation for treatment of early breast cancer: a randomised trial. Lancet Oncol 2008;9:331-41.
65. START Trialists' Group, Bentzen SM, Agrawal RK, et al. The UK Standardisation of Breast Radiotherapy (START) Trial B of radiotherapy hypofractionation for treatment of early breast cancer: a randomised trial. Lancet 2008;371:1098-107.
66. Yarnold J, Ashton A, Bliss J, et al. Fractionation sensitivity and dose response of late adverse effects in the breast after radiotherapy for early breast cancer: long-term results of a randomised trial. Radiother Oncol 2005;75:9-17.
67. Liu Q, Schneider F, Ma L, et al. Relative Biologic Effectiveness (RBE) of 50 kV X-rays Measured in a Phantom for Intraoperative Tumor-Bed Irradiation. Int J Radiat Oncol Biol Phys 2013;85:1127-33.
68. Bistrović M, Bisćan M, Viculin T. RBE of 20 kV and 70 kV X-rays determined for survival of V 79 cells. Radiother

 

Oncol 1986;7:175-80.
69. Hoshi M, Antoku S, Nakamura N, et al. Soft X-ray dosimetry and RBE for survival of Chinese hamster V79 cells. Int J Radiat Biol 1988;54:577-91.
70. Spadinger I, Palcic B. The relative biological effectiveness of 60Co gamma-rays, 55 kVp X- rays, 250 kVp X-rays, and 11 MeV electrons at low doses. Int J Radiat Biol 1992;61:345-53.
71. Raju MR, Carpenter SG, Chmielewski JJ, et al. Radiobiology of ultrasoft X rays. I. Cultured hamster cells (V79). Radiat Res 1987;110:396-412.
72. Goodhead DT. Inactivation and mutation of cultured mammalian cells by aluminium characteristic ultrasoft X-rays. III. Implication for theory of dual radiation action. Int J Radiat Biol Relat Stud Phys Chem Med 1977;32:43-70.
73. Jones B. The apparent increase in the {beta}-parameter of the linear quadratic model with increased linear energy transfer during fast neutron irradiation. Br J Radiol 2010;83:433-6.
74. Brown JM, Koong AC. High-dose single-fraction radiotherapy: exploiting a new biology? Int J Radiat Oncol Biol Phys 2008;71:324-5.
75. Herskind C, Ma L, Liu Q, et al. Biological Effect of Single, Very Large Dose Fractions as Used in Intraoperative Radiotherapy (IORT). World Congress on Medical Physics and Biomedical Engineering, September 7-12, 2009, Munich, Germany. IFMBE Proceedings 2009;25/III:18-21.
76. Herskind C, Wenz F. Is There More to Intraoperative Radiotherapy Than Physical Dose?. Int J Radiat Oncol Biol Phys 2009;74:976-7.
77. Goodhead DT. Saturable repair models of radiation action in mammalian cells. Radiat Res Suppl 1985;8:S58-67.
78. Rothkamm K, Lobrich M. Evidence for a lack of DNA double-strand break repair in human cells exposed to very low x-ray doses. Proc Natl Acad Sci USA 2003;100:5057-62.
79. Astrahan M. Some implications of linear-quadratic-linear radiation dose-response with regard to hypofractionation. Med Phys 2008;35:4161-72.
80. Veldwijk MR, Zhang B, Wenz F, et al. The biological effect of large single doses: a possible role for non-targeted effects in cell inactivation. PLoS One 2014. doi: 10.1371/journal.pone.0084991.
81. Blyth BJ, Sykes PJ. Radiation-induced bystander effects: what are they, and how relevant are they to human radiation exposures? Radiat Res 2011;176:139-57.
82. Garcia-Barros M, Paris F, Cordon-Cardo C, et al. Tumor response to radiotherapy regulated by endothelial cell apoptosis. Science 2003;300:1155-9.
83. Rotolo JA, Maj JG, Feldman R, et al. Bax and Bak do not exhibit functional redundancy in mediating radiation-induced endothelial apoptosis in the intestinal mucosa. Int J Radiat Oncol Biol Phys 2008;70:804-15.
84. Truman JP, García-Barros M, Kaag M, et al. Endothelial membrane remodeling is obligate for anti-angiogenic radiosensitization during tumor radiosurgery. PLoS One 2010;5.
85. Ch'ang HJ, Maj JG, Paris F, et al. ATM regulates target switching to escalating doses of radiation in the intestines. Nat Med 2005;11:484-90.
86. Rotolo JA, Mesicek J, Maj J, et al. Regulation of ceramide synthase-mediated crypt epithelium apoptosis by DNA damage repair enzymes. Cancer Res 2010;70:957-67.
87. Mesicek J, Lee H, Feldman T, et al. Ceramide synthases 2, 5, and 6 confer distinct roles in radiation-induced apoptosis in HeLa cells. Cell Signal 2010;22:1300-7.
88. Park JW, Park WJ, Futerman AH. Ceramide synthases as potential targets for therapeutic intervention in human diseases. Biochim Biophys Acta 2013. [Epub ahead of print].
89. Schiffmann S, Sandner J, Birod K, et al. Ceramide synthases and ceramide levels are increased in breast cancer tissue. Carcinogenesis 2009;30:745-52.
90. Wang J, Boerma M, Fu Q, et al. Significance of endothelial dysfunction in the pathogenesis of early and delayed radiation enteropathy. World J Gastroenterol 2007;13:3047-55.
91. Maeda A, Leung MK, Conroy L, et al. In vivo optical imaging of tumor and microvascular response to ionizing radiation. PLoS One 2012;7:e42133.
92. Finkelstein SE, Timmerman R, McBride WH, et al. The confluence of stereotactic ablative radiotherapy and tumor immunology. Clin Dev Immunol 2011;2011:439752.
93. Formenti SC, Demaria S. Radiation therapy to convert the tumor into an in situ vaccine. Int J Radiat Oncol Biol Phys 2012;84:879-80.
94. Kaur P, Asea A. Radiation-induced effects and the immune system in cancer. Front Oncol 2012;2:191.
95. Reits EA, Hodge JW, Herberts CA, et al. Radiation modulates the peptide repertoire, enhances MHC class I expression, and induces successful antitumor immunotherapy. J Exp Med 2006;203:1259-71.
96. Lugade AA, Sorensen EW, Gerber SA, et al. Radiation-induced IFN-gamma production within the tumor microenvironment influences antitumor immunity. J Immunol 2008;180:3132-9.
97. Demaria S, Bhardwaj N, McBride WH, Formenti SC. Combining radiotherapy and immunotherapy: a revived partnership. Int J Radiat Oncol Biol Phys 2005;63:655-66.
98. Demaria S, Formenti SC. Radiation as an immunological adjuvant: current evidence on dose and fractionation.

 

Front Oncol 2012;2:153.
99. Lugade AA, Moran JP, Gerber SA, et al. Local radiation therapy of B16 melanoma tumors increases the generation of tumor antigen-specific effector cells that traffic to the tumor. J Immunol 2005;174:7516-23.
100. Lee Y, Auh SL, Wang Y, et al. Therapeutic effects of ablative radiation on local tumor require CD8+ T cells: changing strategies for cancer treatment. Blood 2009;114:589-95.
101. Kachikwu EL, Iwamoto KS, Liao YP, et al. Radiation enhances regulatory T cell representation. Int J Radiat Oncol Biol Phys 2011;81:1128-35.
102. Schaue D, Ratikan JA, Iwamoto KS, et al. Maximizing tumor immunity with fractionated radiation. Int J Radiat Oncol Biol Phys 2012;83:1306-10.
103. Belletti B, Vaidya JS, D'Andrea S, et al. Targeted intraoperative radiotherapy impairs the stimulation of breast cancer cell proliferation and invasion caused by surgical wounding. Clin Cancer Res 2008;14:1325-32.
104. Vaidya JS, Joseph DJ, Tobias JS, et al. Targeted intraoperative radiotherapy versus whole breast radiotherapy for breast cancer (TARGIT-A trial): an international, prospective, randomised, non-inferiority phase 3 trial. Lancet 2010;376:91-102.
105. Tagliabue E, Agresti R, Carcangiu ML, et al. Role of HER2 in wound-induced breast carcinoma proliferation. Lancet 2003;362:527-33.
106. Van Dyk J, Keane TJ, Kan S, et al. Radiation pneumonitis following large single dose irradiation: a re- evaluation based on absolute dose to lung. Int J Radiat Oncol Biol Phys 1981;7:461-7.
107. Herskind C, Wenz F. Radiobiological comparison of hypofractionated accelerated partial-breast irradiation (APBI) and single-dose intraoperative radiotherapy (IORT) with 50-kV X-rays. Strahlenther Onkol 2010;186:444-51.
108. Dörr W, van der Kogel AJ. The volume effect in radiotherapy. In: Joiner M, van der Kogel AJ. eds. Basic Clinical Radiobiology. Fourth. ed. London: Hodder Arnold, 2009:191-206.
109. Blank E, Kraus-Tiefenbacher U, Welzel G, et al. Single-center long-term follow-up after intraoperative radiotherapy as a boost during breast-conserving surgery using low-kilovoltage x-rays. Ann Surg Oncol 2010;17:352-8.
110. Kraus-Tiefenbacher U, Bauer L, Scheda A, et al. Long-term toxicity of an intraoperative radiotherapy boost using low energy X-rays during breast-conserving surgery. Int J Radiat Oncol Biol Phys 2006;66:377-81.
111. Bartelink H, Horiot JC, Poortmans PM, et al. Impact of a higher radiation dose on local control and survival in breast-conserving therapy of early breast cancer: 10-year results of the randomized boost versus no boost EORTC 22881-10882 trial. J Clin Oncol 2007;25:3259-65.
112. Poortmans P, Bartelink H, Horiot JC, et al. The influence of the boost technique on local control in breast conserving treatment in the EORTC 'boost versus no boost' randomised trial. Radiother Oncol 2004;72:25-33.
113. Sperk E, Welzel G, Keller A, et al. Late radiation toxicity after intraoperative radiotherapy (IORT) for breast cancer: results from the randomized phase III trial TARGIT A. Breast Cancer Res Treat 2012;135:253-60.
114. Faverly DR, Hendriks JH, Holland R, et al. Breast carcinomas of limited extent: Frequency, radiologic-pathologic characteristics, and surgical margin requirements. Cancer 2001;91:647-59.
115. Huang E, Buchholz TA, Meric F, et al. Classifying local disease recurrences after breast conservation therapy based on location and histology: new primary tumors have more favorable outcomes than true local disease recurrences. Cancer 2002;95:2059-67.
116. Herskind C, Griebel J, Kraus-Tiefenbacher U, et al. Sphere of equivalence--a novel target volume concept for intraoperative radiotherapy using low-energy X rays. Int J Radiat Oncol Biol Phys 2008;72:1575-81.
117. Huang J, Barbera L, Brouwers M, et al. Does delay in starting treatment affect the outcomes of radiotherapy? A systematic review. J Clin Oncol 2003;21:555-63.
118. Vaidya JS, Wenz F, Bulsara M, et al. Risk-adapted targeted intraoperative radiotherapy versus whole-breast radiotherapy for breast cancer: 5-year results for local control and overall survival from the TARGIT-A randomised trial. Lancet 2014;383:603-13.
119. Grantzau T, Mellemkjaer L, Overgaard J. Second primary cancers after adjuvant radiotherapy in early breast cancer patients: a national population based study under the Danish Breast Cancer Cooperative Group (DBCG). Radiother Oncol 2013;106:42-9.
120. Aziz MH, Schneider F, Clausen S, et al. Can the risk of secondary cancer induction after breast conserving therapy be reduced using intraoperative radiotherapy (IORT) with low-energy x-rays? Radiat Oncol 2011;6:174.

**Cite this article as:** Herskind C, Wenz F. Radiobiological aspects of intraoperative tumour-bed irradiation with low-energy X-rays (LEX-IORT). Transl Cancer Res 2014;3(1):3-17. doi: 10.3978/j.issn.2218-676X.2014.01.06